Journal of the Ceramic Society of Japan 110 [10] 911-915 (2002)

Paper

Low-Temperature Synthesis of Single-Phase Lead Zirconate Titanate Thin Film with a nm-Seeding Technique

Tomokazu TANASE, Ayako NISHIKATA, Yusuke IIZUKA, Yoshio KOBAYASHI, Mikio KONNO and Takao MIWA*

Department of Chemical Engineering, Graduate School of Engineering, Tohoku University, Aoba, Aramaki-aza, Aoba-ku, Sendai-shi 980-8579
**Hitachi Research Laboratory, Hitachi, Ltd., 7-1-1, Omika-cho, Hitachi-shi 319-1292*

チタン酸バリウムストロンチウムナノ粒子添加によるチタン酸ジルコン酸鉛薄膜の低温結晶化

棚瀬智和・西片亜矢子・飯塚祐介・小林芳男・今野幹男・三輪崇夫*

東北大学大学院工学研究科，980-8579 仙台市青葉区荒巻字青葉 07
*日立製作所日立研究所，319-1292 日立市大みか町 7-1-1

Ferroelectric lead zirconate titanate (PZT) thin films containing crystalline seeds of barium strontium titanate (BST) nanoparticles were prepared by the complex alkoxide precursor method on indium titanium oxide (ITO) glass electrodes. The PZT films approximately 500 nm thick at BST particle concentrations of 0-34.2 mol% were fabricated with a spin-coating method and annealed at various temperatures. A non-seeded PZT film was crystallized into a perovskite structure by annealing at 500°C. The seeding with the BST particles promoted crystalline growth of PZT perovskite around the seeds, and lowered the crystallization temperature of the PZT films to 420°C. [Received April 11, 2002; Accepted July 11, 2002]

Key-words : *Lead zirconate titanate, Barium strontium titanate, Nanoparticle, Thin film, Sol-gel method, Perovskite, Crystallization temperature*

1. Introduction

Increasing attention is being directed toward ferroelectric films because of their wide range of applications in the case of electronic devices such as non volatile memory, pyro- and piezo-electric sensors and microactuators.[1)-4)] PZT is a typical ferroelectric material that has been studied extensively due to its excellent electrical properties. Fabrication of ferroelectric films includes the use of techniques such as sputtering,[5)-9)] pulsed laser deposition,[10)-13)] chemical vapor deposition[14)-17)] and the sol-gel technique.[18)-32)] Among these techniques, the sol-gel one is a good candidate as a future process, because it is a low-temperature synthesis method and it is easy to attain homogeneous compositions.

As-prepared PZT films generally have amorphous structures and require annealing at high temperatures of more than 500°C to crystallize the products into perovskite structures.[33),34)] Development of crystallization processes that occur at lower temperatures is important not only for saving energy but also for avoiding volatilization of PbO, thermal stresses and interdiffusion between the PZT film and electrode/substrate.[35)-37)] In addition, low-temperature processes have the advantage of preventing thermal annealing from damaging substrate electrodes.

To lower the crystallization temperature, a number of attempts have been made such as rapid heating of the amorphous film,[38)] interlayer deposition between the substrate and film,[33),34)] high-pressure annealing[39)] and the use of substrate materials with appropriate lattice parameters similar to those of the crystalline PZT.[40)] Wu and coworkers studied the seeding effects on crystallization of PZT films employing the powders of PZT and barium titanate (BT) as seeds.[36),37)] The powders were synthesized with a sol-gel method, dried and redispersed in a precursor solution of PZT complex alkoxide. The seeding process was found to improve the crystallization of the films.

In this research, we studied the seeding effects with the use of barium strontium titanate (BST) crystalline nanoparticles employing a simple method that requires neither drying-redispersion nor the use of redispersants. Suspensions of the BST particles prepared with a sol-gel method were directly mixed with a precursor solution for fabrication with spin-coating. The fabricated films were analyzed with XRD analysis after annealing at various temperatures.

2. Experimental

2.1 Materials

Starting reagents were metallic barium (Kanto Chemical Co.), strontium (Kanto Chemical Co.), tetraethylorthotitanate (TEOT) (Tokyo Kasei Kogyo Co., 97%), lead (II) acetate (Kojundo Chemical Lab., 99.999%), zirconium (IV) butoxide (Wako Pure Chemical Ind., 85% 1-butanol solution) and titanium tetraisopropoxide (Wako Pure Chemical Ind., 99%). Special grade reagents (Wako Pure Chemical Ind.) of ethanol (99.5%), benzene (99.8%), 2-methoxyethanol (99.0%) and acetylacetone (99.0%) were used as solvent. Indium titanium oxide (ITO) glass (Furuuchi Chemicals) was used as a substrate electrode. Water was distilled and deionized to have an electrical resistance higher than 18 MΩ cm^{-1}.

2.2 Synthesis

2.2.1 BST particles

A complex alkoxide of barium-strontium-titanium was prepared as a precursor of BST particles. At first, a solution (10^{-4} m^3) that dissolved metallic barium (5 mmol) and strontium (5 mmol) in a 50% (v/v) ethanol/benzene cosolvent was refluxed at 73°C for 1 h. Then, TEOT (10 mmol) was added to the solution, which was refluxed for another 1-24 h, and a transparent complex alkoxide was obtained. To hydrolyze the complex alkoxide, the solution was mixed with an equal volume (10^{-4} m^3) of an ethanol/water mixture, and kept at 70°C for 10 h. The solution turned opaque indicating the formation of the BST particles. In the reac-

tions, water concentration was varied from 1 to 20 kmol/m^3.

2.2.2 PZT films

PZT complex alkoxide was prepared with a sol-gel method employing a solvent of 85% (v/v) 2-methoxyethanol/acetyl acetone mixture. According to the literature,[41)-43)] glycol groups of 2-methoxyethanol have a strong affinity with metal atoms in the complex alkoxide, and acetyl acetone can form chelates with ionic metals in solution. The interaction and the chelation are known to reduce the hydrolysis rate of the complex alkoxide.[41)] In addition, 2-methoxyethanol can improve the wettability of an alkoxide solution on an ITO substrate.

For preparation of the PZT complex alkoxide, lead acetate anhydride, zirconium (IV) butoxide and TEOT were dissolved in the 85% (v/v) 2-methoxyethanol/acetyl acetone mixture at a molar ratio of 1 : 0.5 : 0.5 and a total concentration of 1.0 kmol/m^3. This mixture was refluxed at 120°C for 24 h to yield a brownish PZT complex alkoxide, which was mixed with the BST particles that were washed with the 85% (v/v) 2-methoxyethanol/acetyl acetone mixture. The molar ratio of BST to PZT was varied from 1.2 to 34.2% for various amounts of PZT and BST. To fabricate the BST-seeded PZT films, the solution of PZT and BST was spread onto the ITO glass with a spin coater at 2000 rpm for 30 s and dried at 200°C for 1 min. The spin-coating and drying processes were repeated five times. The fabricated films were heated in air at 380–540°C for 1 h.

2.3 Measurements

BST particles and the films were characterized by transmission electron microscopy (TEM), a scanning electron microscope (SEM), X-ray diffraction (XRD) and optical microscopy. TEM was performed with a Zeiss LEO 912 OMEGA microscope operating at 100 kV. Samples for TEM were prepared by dropping and evaporating the particle suspensions on top of a collodion-coated copper grid. The films were sputtered with Pt–Pd and observed with a SEM (Zeiss LEO 1420 microscope) operating at 15 kV. XRD (Mac Science, M18XHF^{22}-SRA) measurements were carried out at 50 kV and 200 mA with Mo Kα radiation using a monochromator.

3. Results and discussion

3.1 BST particles

Figures 1 and 2 show TEM images and XRD patterns of the BST particles obtained in the hydrolysis reaction at a water concentration of 20 kmol/m^3 for different reflux times. As the reflux time increased, smaller BST particles appeared, although some particles with sizes of around 30 nm were formed at the reflux time of 24 h. On the other hand, no large difference was observed in the XRD patterns of the particles for the various reflux times. All peaks in the XRD patterns could be clearly attributed to the $Ba_{0.5}Sr_{0.5}TiO_3$ perovskite structure.[44)-46)] Peak intensity scarcely changed with the reflux time. According to Kezuka et al.,[47)] an increase in reflux time can be expected to generate oligomers of complex alkoxides that have large molecular weight. The difference in molecular weight might bring about differences in particle size distribution. However, crystallinity of the particles might not strongly depend on the molecular weight of the oligomers that have a similar composition.

Figure 3 shows TEM images of the BST particles prepared at various water concentrations at a reflux time of 24 h. Sizes of the particles were within 18 ± 5 nm at 4 kmol/m^3 and 32 ± 6 nm at 12 kmol/m^3. At a water concentration of 20 kmol/m^3, a large number of tiny particles appeared together with a small number of large particles.

The XRD patterns of the BST particles of Fig. 3 are shown in Fig. 4. The as-prepared BST particles crystallized without the need for any further heat treatment. Average grain sizes for particles prepared at water concentrations of 4, 12 and 20 kmol/m^3 were estimated from the X-ray diffraction line broadening of the (110) peak according to the Scherrer equation as 8.3, 13.9 and 9.5 nm, respectively. The appearance of the maximum grain size corresponded to the change in average particle size in Fig. 3. The sizes of grains and particles are evidence that the BST particles were composed of several BST grain units. An increase in peak intensity with water concentration can be seen in

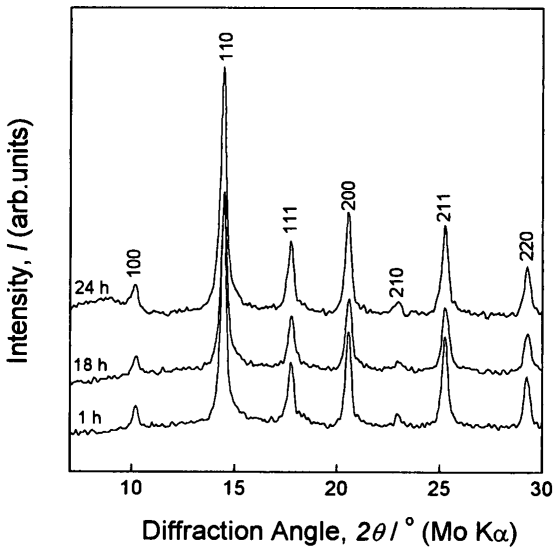

Fig. 2. XRD patterns of BST particles. Precursor complex alkoxide of BST particles was prepared by refluxing at 73°C for 1, 18 and 24 h. Water concentration was 20 kmol/m^3.

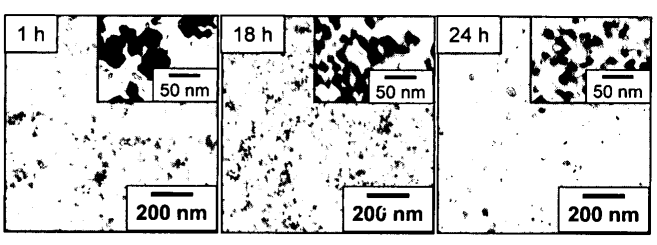

Fig. 1. TEM images of BST particles. Precursor complex alkoxide of BST particles was prepared by refluxing at 73°C for 1, 18 and 24 h. Water concentration was 20 kmol/m^3. A photograph taken at a higher magnification is shown in each inset.

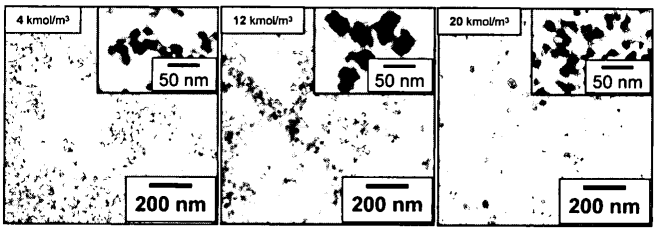

Fig. 3. TEM images of BST particles. The precursor complex alkoxide was hydrolyzed at water concentrations of 4, 12 and 20 kmol/m^3. Precursor complex alkoxide of BST particles was prepared by refluxing at 73°C for 24 h. A photograph taken at higher magnification is shown in each inset.

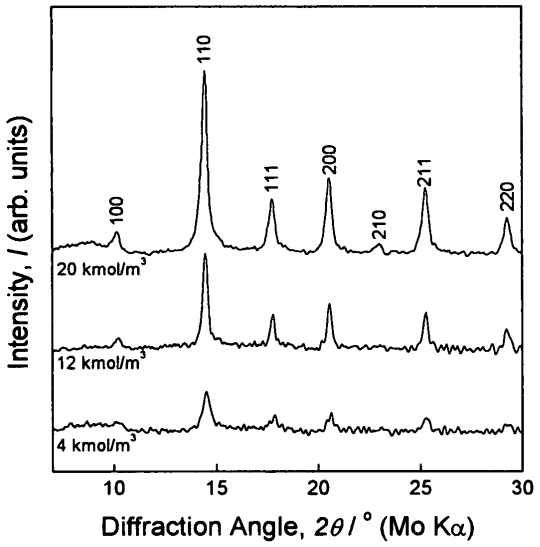

Fig. 4. XRD patterns of BST particles. See Fig. 3 for reaction conditions.

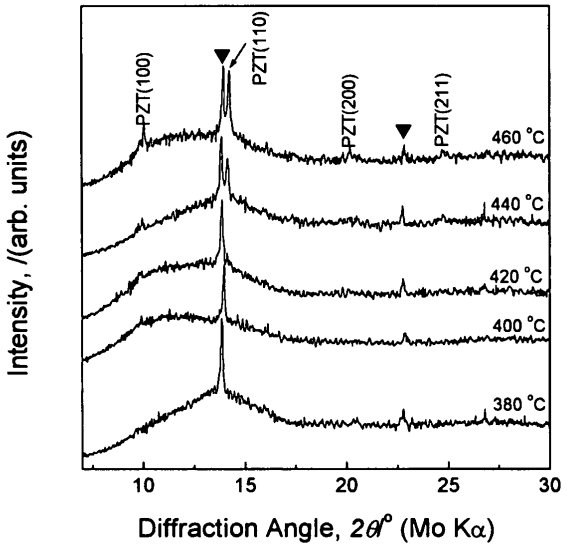

Fig. 6. XRD patterns of 1.2 mol% BST-seeded PZT films. Symbol: ▼ ITO substrate.

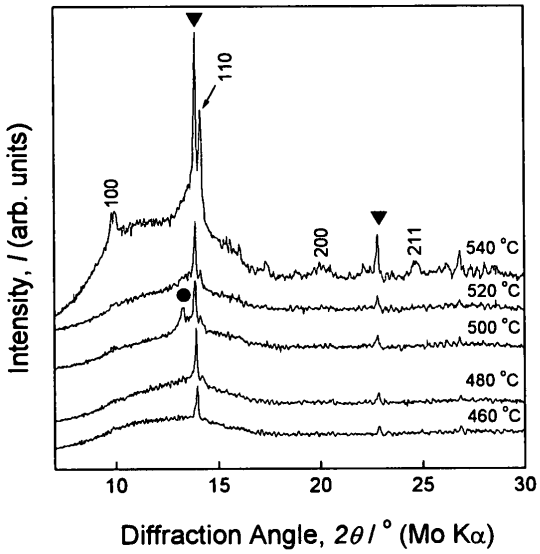

Fig. 5. XRD patterns of non-seeded PZT films. Symbols: ▼ ITO substrate, ● PZT pyrochlore phase.

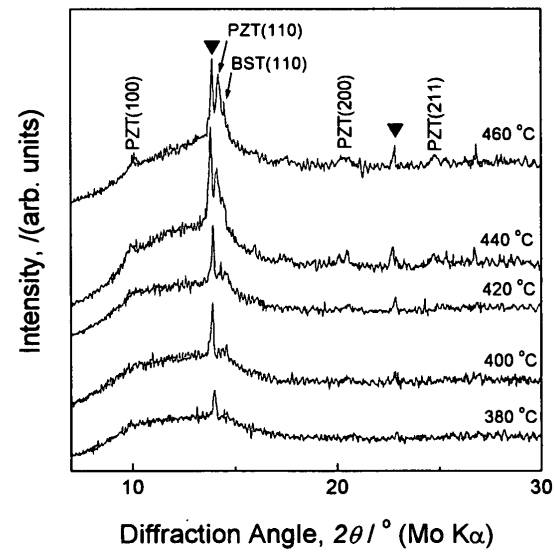

Fig. 7. XRD patterns of 34.2 mol% BST-seeded PZT films. Symbol: ▼ ITO substrate.

Fig. 4 and thus indicates the development of crystallization, which probably results from the promotion of hydrolysis and condensation of the complex alkoxide. However, when the water concentration was raised to above 20 kmol/m^3, no particles were obtained but a viscous or solid gel was formed from the complex alkoxide.

3.2 PZT films

The BST particles with the highest crystallinity obtained at the water concentration of 20 kmol/m^3 were used to fabricate the PZT films. In the fabrication, the spin-coating speed was varied to change film thickness. Each coating thickness was controlled to be less than 100 nm, to avoid damage due to thermal shrinkage. The total thickness of the final film with five coating layers was about 500 nm.

Figures 5, 6 and 7 show XRD patterns of non-, 1.2 mol% BST- and 34.2 mol% BST-seeded PZT films at various annealing temperatures. In the non-seeded films (Fig. 5), a few peaks began to appear at 500°C. The peak observed at 13.3° for the 500°C-annealed film can be attributed to the pyrochlore phase of PZT,[19),48)] which is, in general, detrimental to the electrical and mechanical characteristics of films.[49)] After annealing above 500°C, the pyrochlore peak disappeared and several peaks appeared that were indicative of the presence of PZT perovskite. These peak intensities increased with the annealing temperature, indicating progression of the PZT crystallinity. In Fig. 6, PZT perovskite peaks first appeared at 420°C and intensified with the annealing temperature. No peaks due to a pyrochlore phase were observed for the BST-seeded PZT films over the entire range of annealing temperatures considered, although it has been reported that a pyrochlore phase appeared in PZT-seeded and BT-seeded PZT films even after high-temperature annealing at 500°C.[36),37)] As shown in Fig. 7, the absence of pyrochlore formation was also observed in the 34.2 mol% BST-seeded PZT films.

An important factor in crystalline growth is the similarity

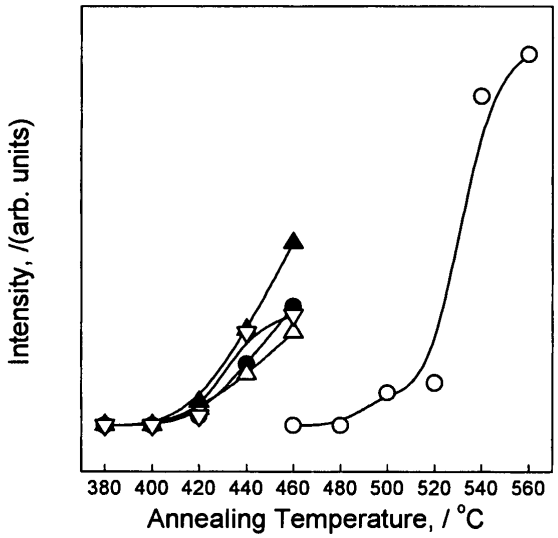

Fig. 8. XRD peak intensity versus annealing temperature at 0 (○), 1.2 (●), 6.0 (△), 11.9 (▲) and 34.2 mol% (▽) of BST concentrations. The peak intensity was obtained from the area of the (110) peak.

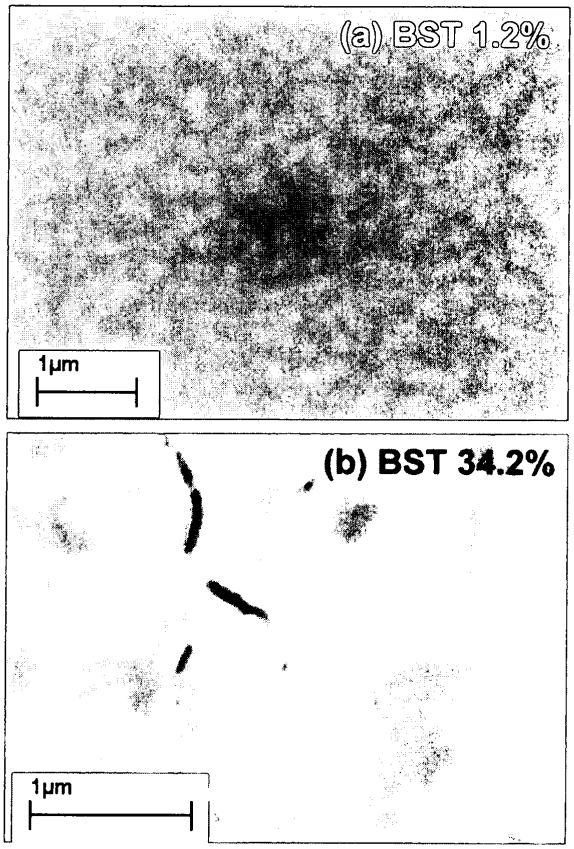

Fig. 9. SEM images of PZT films seeded with (a) 1.2 mol% and (b) 34.2 mol% of BST nanoparticles. Both the films were annealed at 460°C for 1 h.

of the crystal lattice constants. The (110) peaks were employed to discuss the crystallization because of their strong diffraction intensity. The (110) *d*-spacing values of the BT and PZT perovskites are 0.283 nm and 0.287 nm, both of which are closer to the value for PZT pyrochlore (0.302 nm) than that for the BST perovskite (0.279 nm). Therefore, seeds of the BT and PZT perovskites should have a higher possibility to promote pyrochlore formation than the BST seed. In other words, the *d*-spacing of the BST is far from that of the PZT pyrochlore but close to that of the PZT perovskite. This seems to be the reason for the apperance of the simple phase PZT perovskite in the present work. In Fig. 6, the peak of the BST was scarcely observed because of the low content of the BST. However, in Fig. 7, due to the high content of the BST the BST peak was revealed.

Figure 8 shows the dependence of XRD peak intensities of PZT perovskite (110) on annealing temperature. The crystallization temperature of the seeded films did not seem to strongly depend on the concentration of the BST particles, while the incorporation of the BST seeds into the PZT film lowered the crystallization temperature from 500°C (the non-seeded PZT) to 420°C.

Figure 9 shows SEM images of the PZT films containing 1.2 and 34.2 mol% of BST. Cracks, peeling-off, layer separation and other defects were not observed for the 1.2 mol% BST seeded PZT film. White dots having a size of around 150 nm were dispersed uniformly and could be the grown PZT grains. Similar SEM images were also obtained for 6.0 and 11.9 mol%-seeded PZT films. In contrast, for samples prepared from 34.2 mol% BST and annealed at 460°C, some scratch-type cracks were observed on the surface. This may be due to the excessive addition of BST that would increase the thermal stress due to a difference in thermal shrinkage between the PZT film and the BST particles.

4. Conclusions

PZT films seeded with 1.2–34.2 mol% of BST particles were crystallized at 420°C to generate perovskite structures. The seeding of the BST particles was found to lower the required crystallization temperature and prevent the formation of PZT pyrochlore phase, producing the PZT single phase. Crack-free and smooth surfaces were attained for annealed PZT films with 1.2, 6.0 and 11.9 mol% of BST particles.

References

1) Scott, J. F. and Paz de Araujo, C. A., *Science*, **246**, 1400–05 (1989).
2) Morten, B., De Cicro, G. and Prudenziati, M., *Sensors and Actuators A*, **31**, 153–58 (1992).
3) Mathews, S., Ramesh, R., Venkatesan, T. and Benedetto, J., *Science*, **276**, 238–40 (1997).
4) Ding, A.-L., Luo, W.-G., Qiu, P. S., Feng, J. W. and Zhang, R. T., *J. Mater. Res.*, **13**, 1266–70 (1998).
5) Bouregba, R., Poullain, G., Vilquin, B. and Murray, H., *Mater. Res. Bull.*, **35**, 1381–90 (2000).
6) Kim, J.-D., Sasaki, K. and Hata, T., *Vacuum*, **59**, 559–66 (2000).
7) Li, X.-S., Yamashita, K., Tanaka, T., Suzuki, Y. and Okuyama, M., *Sensors and Actuators A*, **82**, 265–69 (2000).
8) Lee, J. Y. and Lee, B. S., *Mater. Sci. Eng.*, **B79**, 86–89 (2001).
9) Masuda, T., Miyaguchi, Y., Tanimura, M., Nishioka, Y., Suu, K. and Tani, N., *Appl. Suf. Sci.*, **169–170**, 539–43 (2001).
10) Guerrero, C., Ferrater, C., Roldán, J., Trtík, V., Sánchez, F. and Varela, M., *Microelectronics Reliability*, **40**, 671–74 (2000).
11) Fujita, H., Imade, M., Sakashita, M., Sakai, A., Zaima, S. and Yasuda, Y., *Appl. Suf. Sci.*, **159–160**, 134–37 (2000).
12) Zhao, J., Lu, L., Thompson, C. V., Lu, Y. F. and Song, W. D., *J. Cryst. Growth*, **225**, 173–77 (2001).
13) Kim, S. S., Kim, B. I., Park, Y. B., Kang, T. S. and Je, J. H., *Appl. Suf. Sci.*, **169–170**, 553–56 (2001).
14) Okada, M., Tominaga, K., Araki, T., Katayama, S. and Sakashita, Y., *Jpn. J. Appl. Phys.*, **29**, 718–22 (1990).
15) Lin, J., Chen, H. Y., Tan, K. L. and Feng, Z. C., *Thin Solid Films*, **289**, 59–64 (1996).

16) Peng, C. H. and Desu, S. B., *Appl. Phys. Lett.*, **61**, 16–18 (1992).
17) Wakiya, N., Kuroyanagi, K., Xuan, Y., Shinozaki, K. and Mizutani, N., *Thin Solid Films*, **372**, 156–62 (2000).
18) Wu, A., Yang, L., Vilarinho, P. M., Miranda Salvado, I. M. and Baptista, J. L., *Thin Solid Films*, **365**, 24–28 (2000).
19) Meng, X. J., Cheng, J. G., Sun, J. L., Tan, J., Ye, H. J. and Chu, J. H., *Thin Solid Films*, **368**, 22–25 (2000).
20) Miyazawa, K., Ito, K. and Maeda, R., *Ceram. Inter.*, **26**, 501–06 (2000).
21) Takahashi, Y., *Thin Solid Films*, **370**, 5–9 (2000).
22) Liu, W., Ko, J. S. and Zhu, W., *Thin Solid Films*, **371**, 254–58 (2000).
23) Lee, S.-G., Kim, K. T. and Lee, Y. H., *Thin Solid Films*, **372**, 45–49 (2000).
24) Zhou, Q.-F., Chan, H. L. W. and Choy, C. L., *Thin Solid Films*, **375**, 95–99 (2000).
25) Shi, C., Meidong, L., Churong, L., Yike, Z. and Costa, J. D., *Thin Solid Films*, **375**, 288–91 (2000).
26) Yang, J.-K., Kim, W. S. and Park, H.-H., *Thin Solid Films*, **377–378**, 739–44 (2000).
27) Fu, X., Li, J., Song, Z. and Lin, C., *J. Cryst. Growth*, **220**, 82–87 (2000).
28) Seveno, R., Limousin, P., Averty, D., Chartier, J.-L., Bihan, R. L. and Gundel, H. W., *J. Eur. Ceram Soc.*, **20**, 2025–28 (2000).
29) Pu, X., Luo, W., Ding, A., Tian, H. and Qiu, P., *Mater. Res. Bull.*, **36**, 1471–78 (2001).
30) Cheng, J. and Meng, Z., *Thin Solid Films*, **375**, 5–10 (2001).
31) Es-Souni, M., Abed, M., Piorra, A., Malinowski, S. and Zaporojtchenko, V., *Thin Solid Films*, **389**, 99–107 (2001).
32) Yang, W. D., *Ceram. Inter.*, **27**, 373–84 (2001).
33) Kwok, C. K. and Desu, S. B., *J. Mater. Res.*, **8**, 339–44 (1993).
34) Aoki, K., Fukuda, Y., Numata, K. and Nishimura, A., *Jpn. J. Appl. Phys.*, **34**, 192–95 (1995).
35) Lakeman, C. D. E. and Payne, D. A., *J. Am. Ceram. Soc.*, **75**, 3091–96 (1992).
36) Wu, A., Miranda Salvado, I. M., Vilarinho, P. M. and Baptista, J. L., *J. Eur. Ceram. Soc.*, **17**, 1443–52 (1997).
37) Wu, A., Vilarinho, P. M., Miranda Salvado, I. M. and Baptista, J. L., *Mater. Res. Bull.*, **33**, 59–68 (1998).
38) Chen, J., Udayakumar, K. R., Brooks, K. G. and Cross, L. E., *J. Appl. Phys.*, **71**, 4465–69 (1992).
39) Zeng, J., Zhang, M., Song, Z., Wang, L., Li, J., Li, K. and Lin, C., *Appl. Surf. Sci.*, **148**, 137–41 (1999).
40) Hirano, S., Yogo, T., Kikuta, K., Araki, Y., Saitoh, M. and Ogasahara, S., *J. Am. Ceram. Soc.*, **75**, 2785–89 (1992).
41) Yi, G. and Sayer, M., *Am. Ceram. Soc. Bull.*, **70**, 1173–79 (1991).
42) Giridharan, N. V., Varathaharan, R., Jayavel, R. and Ramasamy, P., *Mater. Chem. Phys.*, **65**, 261–65 (2000).
43) Tursiloadi, S., Imai, H. and Hirashima, H., *J. Ceram. Soc. Japan.*, **103**, 1069–72 (1995).
44) Jang, S.-I. and Jang, H. M., *Ceram. Inter.*, **26**, 421–25 (2000).
45) Wu, D., Li, A., Ling, H., Yin, X., Ge, C., Wang, M. and Ming, N., *Appl. Surf. Sci.*, **165**, 309–14 (2000).
46) López, L. L., Portelles, J., Siqueiros, J. M., Hirata, G. A. and Mckittrick, J., *Thin Solid Films*, **373**, 49–52 (2000).
47) Kezuka, K., Hayashi, Y. and Yamaguchi, T., *J. Am. Ceram. Soc.*, **72**, 1660–63 (1989).
48) Higuchi, K., Miyazaki, K., Sakuma, T. and Suzuki, K., *J. Mater. Sci.*, **29**, 436–41 (1994).
49) Avellaneda, M., Cherkaev, A. V., Lurie, K. A. and Milton, G. W., *J. Appl. Phys.*, **63**, 4989–5003 (1988).